Journal of Leather Science and Engineering

RESEARCH Open Access

Strong synergistic effect of cationic hydrocarbon surfactant and novel nonionic tri-block short-chain fluorocarbon surfactant mixtures on surface activity, wettability and solubilization

Yutang Zhou[1,2], Yong Jin[1,2*], Yichao Shen[1,2], Liangjie Shi[1,2], Shuangquan Lai[1,2] and Yujia Tang[1,2]

Abstract

Mixing hydrocarbon surfactants with fluorocarbon surfactants is still an important strategy to improve the economic benefits and performances of fluorocarbon surfactants and expand their range of application. Herein, we prepared a novel kind of hydrocarbon-fluorocarbon surfactant mixtures via mixing a cationic surfactant, cetyltrimethylammonium bromide (CTAB), with a tri-block nonionic short-chain fluorocarbon surfactant ($F_9EG_{13}F_9$) in aqueous solution. The results showed that adding a small CTAB amount to $F_9EG_{13}F_9$ (the molar fraction of CTAB in the mixture (x_1) was 0.2) could greatly reduce its critical micelle concentrations (*cmc*) from 0.408 mmol/L to 0.191 mmol/L. At this x_1, the contact angle of the mixture was the minimum (57.7 °) at 100 s on polytetrafluoroethylene film, which was even lower than that of $F_9EG_{13}F_9$. Besides, CTAB/$F_9EG_{13}F_9$ mixtures possessed better colloidal stability and solubilization ability toward hydrophobic dye (Sudan I) than $F_9EG_{13}F_9$. The outstanding performances of binary surfactant mixtures benefited from the non-ideal mixing and strong synergistic effect evidence that CTAB/$F_9EG_{13}F_9$ surfactant mixtures could be used in practical applications instead of individual $F_9EG_{13}F_9$, thereby reducing the used cost of $F_9EG_{13}F_9$.

Keywords: Short-chain fluorocarbon surfactant, Hydrocarbon surfactant, Cationic-nonionic mixtures, Surface activity, Wettability, Solubilization

1 Introduction

Fluorocarbon surfactants can be used in leather production to improve the performances and quality of leather due to their outstanding properties, including the wet and dry finishing process of leather production [1–3]. Conventional fluorocarbon surfactants usually have long fluorocarbon chains (C_xF_{2x+1}, $x > 7$). Although them possess many advantages, their serious toxicity and high bioaccumulation in the environment greatly limit their future development [4–7]. For example, a typical finishing agent based on perfluorooctanoic acid (3 M Scotchguard™ FC-805) [8] has been banned. An effective method to decrease the harm to the environment is reducing the number of perfluorinated carbon atoms in a hydrophobic tail from C8-C10 to C4-C6 [9]. Heretofore, a great amount of short-chain fluorocarbon surfactants with low bioaccumulation have been prepared and studied [10–16]. However, the complex synthesis steps and expensive raw materials lead to the high cost of these surfactants, which vastly reduced their range of application. So, how to effectively reduce the used cost of these

* Correspondence: jinyong@cioc.ac.cn
[1]Key Laboratory of Leather Chemistry and Engineering of Ministry of Education, Sichuan University, Chengdu 610065, People's Republic of China
[2]National Engineering Research Center of Clean Technology in Leather Industry, Sichuan University, Chengdu 610065, People's Republic of China

fluorocarbon surfactants is still a hot topic. In fact, a lot of studies have disclosed that binary hydrocarbon surfactant mixtures possessed strong synergistic effect and presented better performances than individual hydrocarbon surfactant such as lower *cmc* [17], stronger solubilization ability and emulsifying ability [18, 19]. Therefore, researchers expect to improve the performances of fluorocarbon surfactants and reduce their high cost by mixing cheap hydrocarbon surfactants with fluorocarbon surfactants [20–22].

Some efforts have been made in recent years to achieve the above objectives. For instance, Wang et al. prepared a kind of fluorocarbon surfactant mixtures with good surface activity by mixing sodium perfluoropolyether carboxylate (PFPE-Na) with cetyltrimethylammonium bromide (CTAB), where the minimum *cmc* of mixtures was 100 times lower than the *cmc* of CTAB and more than 1000 times below that of PFPE-Na [23]. Zhang et al. found that introducing sodium lauryl sulfate (K12) to perfluoropolyether (3) amide propyl dimethyl ammonium iodide (PFPE-A) could effectively decrease the *cmc* of PFPE-A [24]. Jiang et al. reported the foaming ability of mixtures of an amphoteric short-chain fluorocarbon surfactant (FS-50) and sodium dodecyl sulfate (SDS) where the adding of SDS could improve their respective residual foam ratio due to the interaction between two surfactants [25]. Above researches showed the synergistic effect of fluorocarbon and hydrocarbon surfactant mixtures on surface activity and foam ability, ect., which effectively reduced the used cost of fluorocarbon surfactants and improved their performances. However, most of the researches only referred to ionic-ionichydrocarbon-fluorocarbon surfactant mixtures due to the stronger interaction between oppositely charged hydrophilic groups. There was little research on ionic-nonionichydrocarbon-fluorocarbon surfactant mixtures although nonionic fluorocarbon surfactants exhibited the advantages of lower toxicity, stronger salt resistance and stronger acid and alkali resistance [13, 14]. Designing a kind of ionic-nonionichydrocarbon-fluorocarbon surfactant mixture with a strong synergistic effect and good performances is still a challenge.

In this work, we reported a novel class of fluorocarbon surfactant mixtures consisted of cetyltrimethylammonium bromide (CTAB) and a tri-block nonionic fluorocarbon surfactant with two short fluorocarbon chains ($F_9EG_{13}F_9$). Their micellization, adsorption and thermodynamic behaviors were researched via using various theoretical models. Meanwhile, the wettability, colloidal stability and solubilization towards hydrophobic dye of binary mixtures were also investigated. CTAB served as a commercial surfactant commonly is widely used in mixed surfactant systems, and $F_9EG_{13}F_9$ possesses the special tri-block structure that means an adjustable molecular chain spacing [13]. So, the properties of mixtures of CTAB and $F_9EG_{13}F_9$ are intriguing. The results reveal that CTAB/$F_9EG_{13}F_9$ mixtures possess strong synergistic effect, and the performances of binary surfactant mixture with a specific proportion are superior to individual $F_9EG_{13}F_9$ including *cmc*, wettability, colloidal stability and solubilization capacity. We believe that the studying of CTAB/$F_9EG_{13}F_9$ mixtures could provide new insights into the development of fluorocarbon surfactant mixtures with low cost, low bioaccumulation and high performances, which is beneficial to expand the application range of fluorocarbon surfactants in leather and other fields.

2 Materials and methods

2.1 Materials

Cetyltrimethylammonium bromide (CTAB, ≥ 99.0%) and ethanol (≥ 99.7%) were supplied by Kelong Chemical Reagent Factory (Chengdu, China). 1-phenylazo-2-naphthol (Sudan I, ≥ 96.0%) was purchased from Aladdin Chemistry Co., Ltd. (Shanghai, China). All the chemicals were used as received and double distilled water was used in the experiment. The nonionic fluorocarbon surfactant ($F_9EG_{13}F_9$) was synthesized according to the previously reported method [13]. The molecular structures of Sudan I, CTAB and $F_9EG_{13}F_9$ were visualized in Fig. 1.

2.2 Surface tension measurements

Surface tension measurements were performed using an automatic tension meter (BZY-1, Shanghai Hengping Instruments Factory) at 25.0 ± 0.1 °C. The curve of surface tension varying with the logarithm concentration could be obtained via measuring the surface tension of 8–10 different concentrations of sample. Before the measurements of samples with different molar fractions of CTAB, the surface tension of water should also be measured and maintain at about 72.0 mN/m to minimize the experimental error.

2.3 Conductivity measurements

Conductivities of CTAB and its mixtures solutions were measured by using a conductivity analyzer (DDS-11A, Shanghai INESA & Scientific Instrument Co., Ltd., China) at 25 °C. Each sample shall be measured at least six times.

2.4 Contact angle measurements

Dynamic contact angle of individual surfactant or binary mixtures was measured on a DSA 25 contact angle goniometer (Krüss Company, Germany) at 25.0 ± 0.1 °C where the surfactant concentration was 1 mmol/L. The polytetrafluoroethylene (PTFE) film and parafilm were used as base plates.

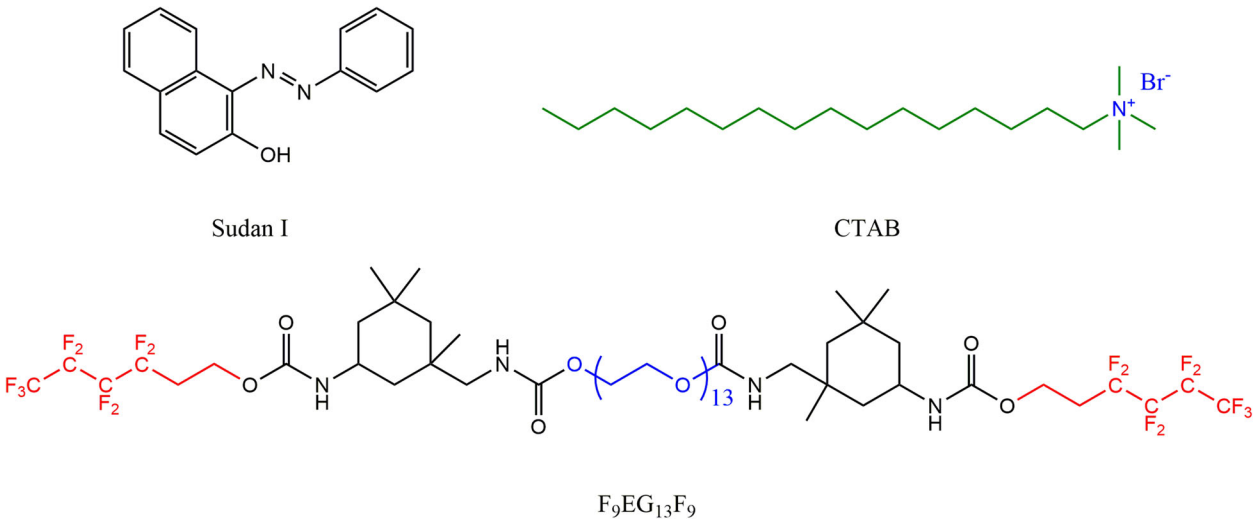

Fig. 1 Molecular structures of Sudan I, CTAB and $F_9EG_{13}F_9$

2.5 Transmittance measurements

Transmittance of CTAB, $F_9EG_{13}F_9$ and their mixture was measured by a Hitachi UV-1900UV-Visible spectrophotometer in the range of visible light range (380 nm–800 nm). The surfactant solutions with a certain concentration (2.5 mmol/L) were prepared and placed in water bath at 25 °C. 2 ml of supernatant was taken for each test.

2.6 Solubilization of hydrophobic dye

To assess the solubilization ability of binary surfactant mixtures towards hydrophobic dye, a series of experiments were carried out by adding an excess of Sudan I to the surfactant solutions with different concentrations to ensure maximum solubility. Subsequently, these samples were stirred for 24 h at 25 °C. Then the excess non-solubilized portion of Sudan I was separated using

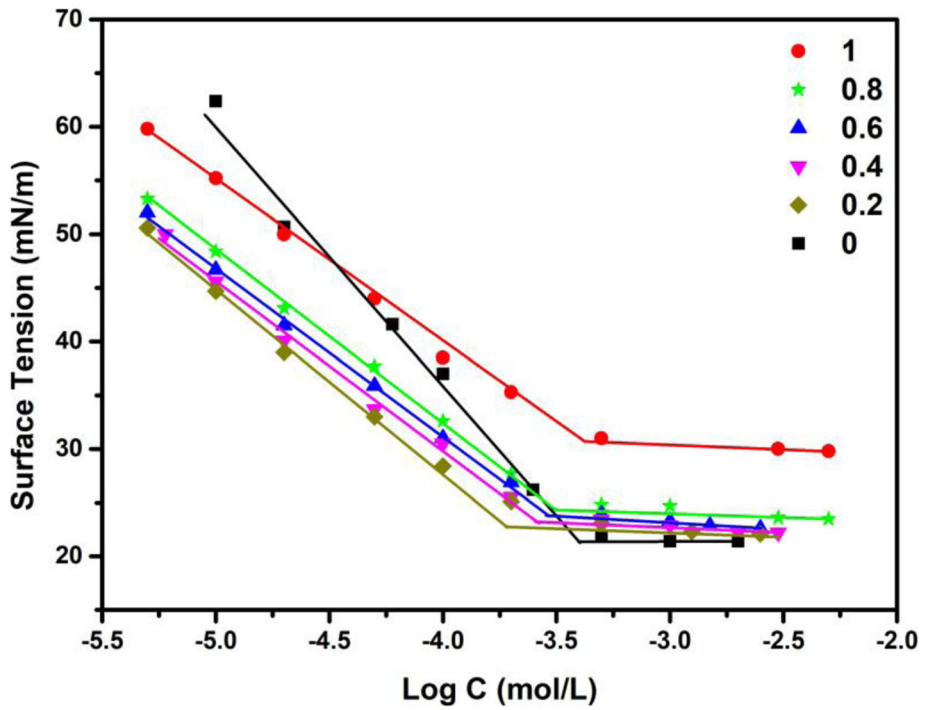

Fig. 2 Variation of surface tension with the logarithm concentration of binary surfactant mixtures at different proportions of CTAB at 25 °C

syringe filters with a Nylon Membrane (pore size of 0.22 μm) and the filtrate (5 mL) was diluted with an equal volume of ethanol. The absorbance of the diluent was measured by a Hitachi UV-1900UV-Visible spectrophotometer at λ_{max} (485 nm) [26]. Besides, the molar absorption coefficient of the Sudan I in ethanol–water (50% v/v) was obtained and its value was 1.1656×10^4 $L \cdot mol^{-1} \cdot cm^{-1}$.

3 Results and discussion

3.1 Micellization behavior of binary mixtures

The curves of surface tension as a function of the logarithm concentration of individual CTAB, $F_9EG_{13}F_9$ and their mixtures were obtained by the surface tension measurements. As depicted in Fig. 2, every curve has an obvious break point which indicates that the micelle has been formed in aqueous solution. And the concentration of surfactant at this point is called critical micelle concentration (*cmc*).

In Table 1, the *cmc* values of CTAB/$F_9EG_{13}F_9$ mixtures are presented. For individual surfactant, the *cmc* value of $F_9EG_{13}F_9$ is 0.408 mmol/L which is consistence with our previous reported date [13]. Whereas, the *cmc* value of CTAB is 0.429 mmol/L which is higher than $F_9EG_{13}F_9$, indicating that $F_9EG_{13}F_9$ is easier to form micelle in a low surfactant concentration. When adding $F_9EG_{13}F_9$ to CTAB, the *cmc* value of CTAB decreases a lot and is even lower than that of $F_9EG_{13}F_9$. It is related to the electrostatic interaction and steric effect between ionic surfactants and nonionic surfactants [27–29]. In our work, the addition of $F_9EG_{13}F_9$ can decrease the electrostatic repulsion effect of cationic hydrophilic head groups of CTAB, meanwhile, the presence of CTAB also decreases the steric hindrance effect of nonionic hydrophilic head groups of $F_9EG_{13}F_9$. With the decrease of molar fraction of CTAB in mixed solution (x_1) from 0.8 to 0.2, the *cmc* values of binary mixtures decrease from 0.314 mmol/L to 0.191 mmol/L indicating that the increase of $F_9EG_{13}F_9$ favors the formation of mixed micelle. Actually, similar phenomenon can be also found in other literatures [30, 31]. This can be ascribed to that the increase of $F_9EG_{13}F_9$ composition enhances the electrostatic screen effect resulting in the weaker electrostatic repulsive force between the cationic hydrophilic head groups of CTAB. Besides, the fluorocarbon surfactant possesses stronger hydrophobicity so that the mixed system with a lower x_1 is more efficient to proceed micellization. The *cmc* values of binary surfactant mixtures with x_1 = 1, 0.8, 0.6, 0.4 and 0.2 measured by conductivity measurements are 0.428, 0.326, 0.298, 0.251 and 0.164 mmol/L, respectively (as represented in Fig. 3), which coincides with those obtained from the surface tension method and indicates the accuracy of the *cmc* values of binary surfactant mixtures. In addition, the conductivity measurements also manifest that the conductivities of solutions decrease with the decrease of x_1, further confirming the electrostatic screen effect of $F_9EG_{13}F_9$.

The *cmc* value of CTAB/$F_9EG_{13}F_9$ mixture on an ideal state can be given by the Clint equation [32].

$$\frac{1}{cmc_{ideal}} = \frac{x_1}{cmc_1} + \frac{1-x_1}{cmc_2} \tag{1}$$

where cmc_{ideal} is the ideal *cmc* value of binary surfactant mixture; cmc_1 and cmc_2 are the *cmc* value of individual CTAB and $F_9EG_{13}F_9$, respectively. Table 1 lists the calculated cmc_{ideal} values and Fig. 4 reveals the difference between the ideal and experimental *cmc* values. As illustrated in Fig. 4, the experimental *cmc* values have an obvious negative deviation from the ideal *cmc* values, suggesting the formation of non-ideal mixtures and the presence of strong interaction between two surfactants due to the decrease of steric hindrance effect and electrostatic repulsion effect.

To further understand the non-ideal behavior for binary surfactant mixtures, Rubingh [33] proposed the well-known regular solution theory (RST). On a basis of RST, the interaction parameter (β_{12}) between CTAB and $F_9EG_{13}F_9$ is given by following equation:

$$\beta_{12} = \frac{\ln[x_1 cmc/(X_1 cmc_1)]}{(1-X_1)^2} \tag{2}$$

where X_1 is the molar fraction of CTAB in the non-ideal mixed micelle, which can be deduced by using Eq. (3)

Table 1 Values of *cmc* and micellization parameters for CTAB/$F_9EG_{13}F_9$ mixtures at different CTAB proportions at 25 °C

x_1	*cmc* (mmol/L)	cmc_{ideal} (mmol/L)	X_1	X_1^{ideal}	f_1	f_2	β_{12}
1	0.429	0.429	1.000	1.000	–	–	–
0.8	0.314	0.425	0.683	0.792	0.857	0.489	−1.532
0.6	0.295	0.420	0.551	0.588	0.749	0.647	−1.435
0.4	0.260	0.416	0.442	0.388	0.548	0.686	−1.929
0.2	0.191	0.412	0.374	0.192	0.238	0.599	−3.662
0	0.408	0.408	0.000	0.000	–	–	–

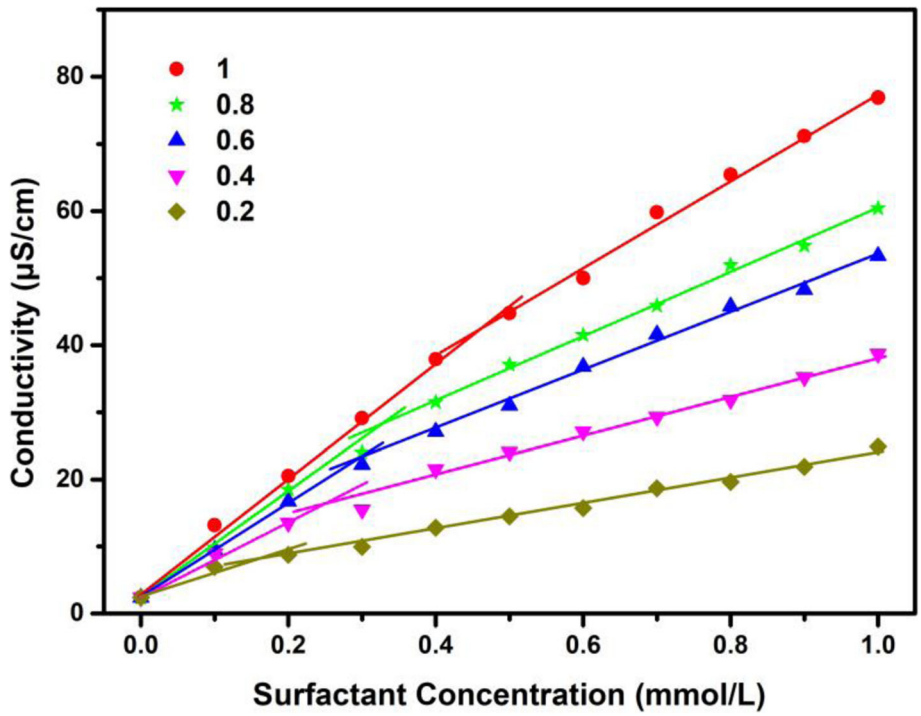

Fig. 3 Variation of conductivity with the concentration of binary surfactant mixtures at different proportions of CTAB at 25 °C

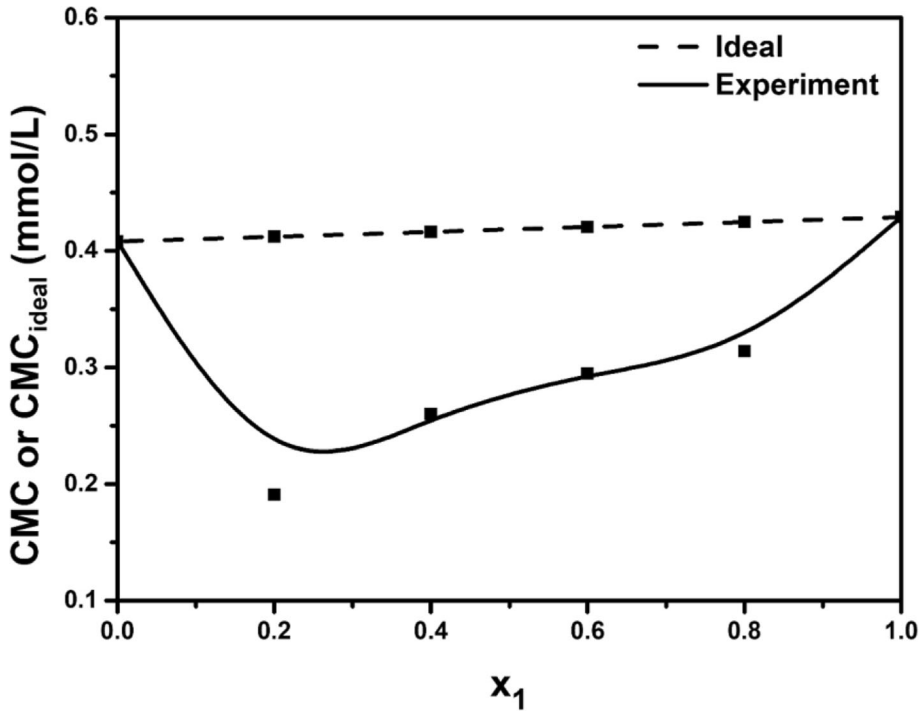

Fig. 4 Comparison between the experimental and ideal *cmc* values of binary surfactant mixtures at different proportions of CTAB at 25 °C

$$\frac{X_1^2 \ln[x_1 cmc/(X_1 cmc_1)]}{(1-X_1)^2 \ln\{\frac{(1-x_1)cmc}{(1-X_1)cmc_2}\}} = 1 \quad (3)$$

Additionally, the molar fraction of CTAB in the ideal mixed micelle (X_1^{ideal}) can be obtained by:

$$X_1^{ideal} = \frac{x_1 cmc_2}{[x_1 cmc_2 + (1-x_1)cmc_1]} \quad (4)$$

The calculated results of above parameters (β_{12}, X_1 and X_1^{ideal}) are given by Table 1. As illustrated in Table 1, the values of X_1 have the deviation from the values of X_1^{ideal} further indicating the formation of non-ideal mixtures. Notably, the negative deviation can be found when the x_1 is in the range of 0.6–0.8 but the positive deviation is presented when the x_1 is less than 0.6. This diffidence can be ascribed to the fact that no matter for CTAB or $F_9EG_{13}F_9$, the high content components always provide an unfavorable factor (the electrostatic repulsion effect or the steric hindrance effect) to hinder the formation of mixed micelles. Therefore, the mixed micelles tend to vary the molar ratio of two surfactants, thereby reducing the hindrance provided by high content components. Subsequently, the interaction degree between CTAB and $F_9EG_{13}F_9$ is estimated by the β_{12}. The negative values of β_{12} are found in all binary mixtures with different x_1, which suggests the presence of strong synergistic effect. At $x_1 = 0.2$, the value of β_{12} reaches the minimum which is − 3.662 and means the strongest synergistic effect. The result is consistent with the measured value of *cmc*.

Moreover, the activity coefficient of CTAB and $F_9EG_{13}F_9$ (denoted as f_1 and f_2, respectively) for the binary mixtures in aqueous solutions can be expressed as Eqs. (5a) and (5b), which describes the degree of participation of two surfactants in the micellization.

$$f_1 = \exp\beta_{12}(1-X_1)^2 \quad (5a)$$

$$f_2 = \exp\beta_{12}X_1^2 \quad (5b)$$

The calculated values of f_1 and f_2 are given in Table 1. It can be observed that f_1 and f_2 are lower than 1.0, further suggesting the non-ideal behavior of binary mixtures. Specially, the f_1 is greater than the f_2 when the x_1 is 0.6–0.8, indicating the formation of the mixed micelles governed by CTAB. Conversely, with the decrease of x_1, $F_9EG_{13}F_9$ replaces CTAB to govern the formation of the mixed micelles. This means that the reduction of adverse factors coursed by high content components is a key point to promote the formation of mixed micelles in CTAB/$F_9EG_{13}F_9$ mixtures.

3.2 Adsorption behavior of binary mixtures

Surfactants possess special amphiphilic structure which enables them to arrange at air-water interface, hydrophilic head in aqueous-phase and hydrophobic tail in air, resulting in the decrease of surface tension of water. Therefore, the measurement of surface tension of surfactant aqueous solution is an important method to characterize its adsorption ability on the water surface. The variation of surface tension with the logarithm concentration of individual CTAB, $F_9EG_{13}F_9$ or their mixtures in aqueous solution was measured by surface tension measurements as depicted in Fig. 2.

Table 2 records the critical surface tension (γ_{cmc}) values of CTAB/$F_9EG_{13}F_9$ mixtures with different x_1. These values mean the surface tension of surfactants aqueous solutions at *cmc* and indicate the saturated molecular arrangement at air-water interface. It can be found in Table 2 that the γ_{cmc} value of $F_9EG_{13}F_9$ (21.4 mN/m) is lower than that of CTAB (30.2 mN/m) because of the strong hydrophobicity of fluorocarbon surfactant. When adding a small $F_9EG_{13}F_9$ amount of to CTAB (x_1 = 0.8), the γ_{cmc} value dramatically decreases from 30.2 mN/m to 24.3 mN/m. It can be attributed to the fact that the special tri-block structure of $F_9EG_{13}F_9$ endows it with an adjustable chain spacing, which means that $F_9EG_{13}F_9$ can screen more cationic head groups of CTAB as depicted in Fig. 5. With further increasing $F_9EG_{13}F_9$, the γ_{cmc} values decrease from 24.3 mN/m to 22.7 mN/m because $F_9EG_{13}F_9$ possesses higher surface activity. Although these binary mixed systems display the strong synergistic effect, their surface activity was hardly on a par with $F_9EG_{13}F_9$. Some possible reasons are implicit in Fig. 5. On the one hand, the exceeded length of hydrocarbon chains may bend and lead to the decrease of interfacial density of fluorocarbon chains. On the other hand, the mutual immiscibility of hydrocarbon and fluorocarbon chains decreases the number of surfactant molecules at air-water interface. Thus, the ability of binary mixtures to reduce surface tension of water is slightly inferior to that of $F_9EG_{13}F_9$.

To further understand the absorption state of individual CTAB, $F_9EG_{13}F_9$ and binary surfactant mixtures on the water surface, two important parameters, the surface

Table 2 Critical surface tension and adsorption parameters for CTAB/$F_9EG_{13}F_9$ mixtures at different CTAB proportions at 25 °C

x_1	γ_{cmc} (mN/m)	$10^6\ \Gamma_{max}$ (mol/m2)	A_{min} (Å^2)	pC_{20}
1	30.2	1.307	127.028	4.83
0.8	24.3	1.422	116.762	5.21
0.6	23.8	1.373	120.919	5.33
0.4	23.2	1.389	119.585	5.40
0.2	22.7	1.513	109.732	5.41
0	21.4	4.198	39.560	4.67

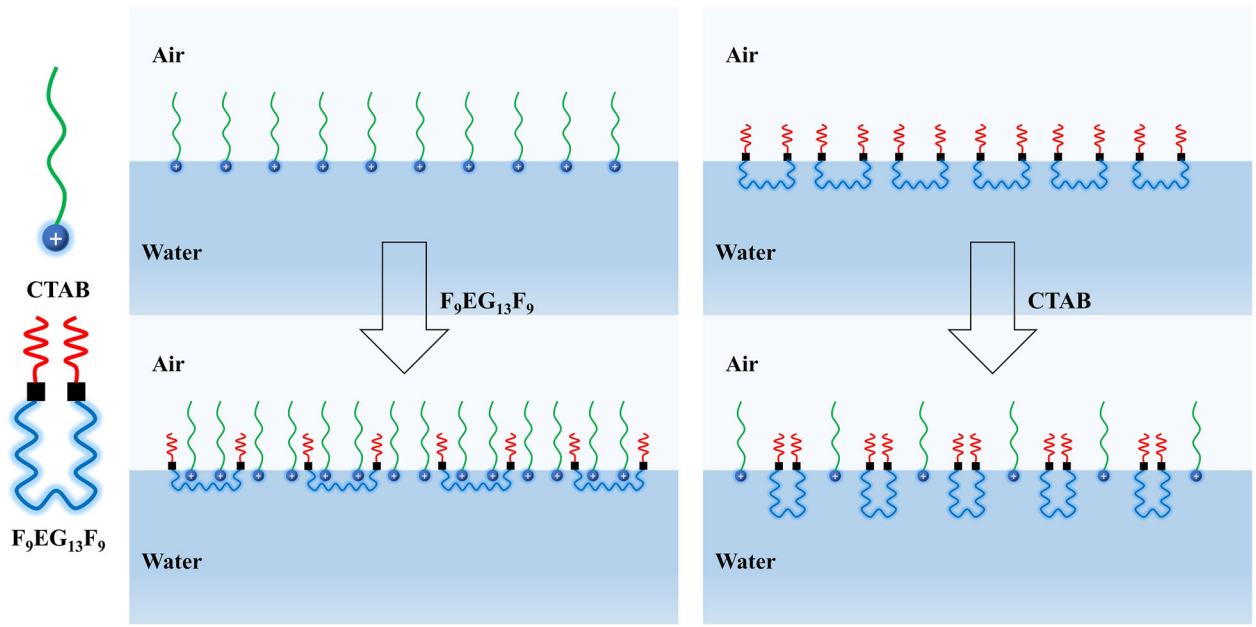

Fig. 5 Variation of molecular arrangement at air-water interface of CTAB (left) and $F_9EG_{13}F_9$ (right) with adding a small amount of another component at 25 °C

excess maximum concentration (Γ_{max}) and average minimum area occupied by per surfactant molecule (A_{min}), are deduced by the following Eqs. (6) to (7).

$$\Gamma_{max} = -\frac{1}{2.303nRT}(\partial\gamma/\partial logC)_T \quad (6)$$

$$A_{min} = 1/(N_A \cdot \Gamma_{max}) \quad (7)$$

where R is the gas constant (8.314 J·mol^{-1}·K^{-1}) and T is the absolute temperature and taken as 298.15 K; $\partial\gamma/\partial logC$ is determined from the maximum slope in Fig. 2; N_A is the Avogadro's constant; the value of n is 1 for nonionic $F_9EG_{13}F_9$ or 2 for cationic CTAB and their mixtures [34, 35]. It can be clear seen the Γ_{max} and A_{min} values of different surfactant systems in Table 2. The higher Γ_{max} values, the lower A_{min} values and the more closely molecular arrangement at air-water interface. Obviously, the Γ_{max} values of binary mixtures are larger than that of CTAB indicating the denser molecular arrangement at air-water interface. With the increase of molar fraction of $F_9EG_{13}F_9$ from 0.2 to 0.4, the Γ_{max} values decrease and A_{min} values increase anomalously due to the increasing repulsive effect between hydrocarbon and fluorocarbon chains adverse to the dense molecular arrangement. Further increasing the molar fraction of $F_9EG_{13}F_9$, the Γ_{max} values increase and the A_{min} values decrease due to the lower A_{min} value of nonionic $F_9EG_{13}F_9$. However, the A_{min} values of CTAB/$F_9EG_{13}F_9$ mixtures are larger than that of $F_9EG_{13}F_9$, which also explains why $F_9EG_{13}F_9$ has better surface activity than its mixtures with CTAB.

Moreover, the adsorption efficiency of CTAB/$F_9EG_{13}F_9$ mixtures with different x_1 is characterized by pC_{20} which is the negative logarithm of surfactant concentration required to reduce the surface tension of water by 20 mN/m [36]. As described in Table 2, the pC_{20} values of CTAB and $F_9EG_{13}F_9$ are 4.83 and 4.67, respectively. Interestingly, the adsorption efficiency of CTAB is slightly superior to that of $F_9EG_{13}F_9$ although $F_9EG_{13}F_9$ possesses stronger hydrophobicity. The reason may be that the nonionic polyoxyethylene chains of $F_9EG_{13}F_9$ are easily twined together, thereby hindering the migration of $F_9EG_{13}F_9$ from solution to air-water interface. For mixed surfactant systems, their pC_{20} values are larger than individual surfactant no matter for CTAB or $F_9EG_{13}F_9$. This is because the presence of CTAB can avoid the entanglement of polyoxyethylene chains and enable $F_9EG_{13}F_9$ to faster adsorb to water surface resulting in the enhancement of interfacial hydrophobicity.

3.3 Thermodynamics of binary mixtures

Thermodynamic behavior of CTAB/$F_9EG_{13}F_9$ mixtures is analyzed via using a series of parameters. For example, the standard free energy of micelle formation (ΔG_{mic}) and adsorption (ΔG_{ads}) for the mixed systems can be calculated from Eq. (8) and Eq. (9) [37, 38], respectively.

$$\Delta G_{\mathrm{mic}} = 2.3RT\ \lg\left(\frac{cmc}{55.3}\right) \tag{8}$$

$$\Delta G_{\mathrm{ads}} = \Delta G_{\mathrm{mic}} - \left(\gamma_0 - \gamma_{cmc}\right)/\Gamma_{\max} \tag{9}$$

where γ_0 is the surface tension of pure water (72.0 mN/m). In addition, to further prove the interaction of CTAB and $F_9EG_{13}F_9$ mixtures, the non-ideal free energy change (ΔG) and ideal free energy change (ΔG_{ideal}) of micellization for binary surfactant mixtures are given by following equations based on the RST [33].

$$\Delta G = RT[X_1\ \ln f_1 X_1 + (1-X_1)\ \ln f_2(1-X_1)] \tag{10}$$

$$\Delta G_{ideal} = RT[X_1\ \ln X_1 + (1-X_1)\ \ln(1-X_1)] \tag{11}$$

The calculated values of thermodynamic parameters are presented in Table 3 that display all negative values indicating the spontaneous micellization and adsorption process of binary surfactant mixtures. Fig. 6 discloses the difference between ΔG_{mic} and ΔG_{ads} values. As shown in Fig. 6, the values of ΔG_{ads} are all lower than the values of ΔG_{mic}, which indicates that the surfactant molecules tend to adsorb at air-water interface rather than form micelles in aqueous solution no matter for individual CTAB, $F_9EG_{13}F_9$ or their mixtures. For the micellization process, the variation trend of ΔG_{mic} values with the decrease of x_1 is consistence with that of *cmc* values. When x_1 is 0.2, the ΔG_{mic} has the minimum value that is − 31.14 KJ/mol. As for adsorption process, ΔG_{ads} values of surfactant mixtures are also lower than those of CTAB (− 61.11 KJ/mol) and $F_9EG_{13}F_9$ (− 41.31 KJ/mol) due to the synergistic effect between two surfactants and the strong hydrophobicity of fluorocarbon surfactant. The calculated results of ΔG and ΔG_{ideal} display the obvious deviation, further suggesting the non-ideal behavior of mixtures.

Furthermore, on a basis of Maeda model proposed in 1995 [39], the thermodynamic stability (ΔG_{M}) of binary ionic/nonionic surfactant mixtures can be obtained by following equation.

$$\Delta G_{\mathrm{M}} = RT\left(B_0 + B_1 X_1 + B_2 X_1^2\right) \tag{12a}$$

where B_0, B_1 and B_2 can be calculated in terms of above dates from the Eqs. (12b) to (12d).

$$B_0 = \ln cmc_2 \tag{12b}$$

$$B_2 = -\beta_{12} \tag{12c}$$

$$\ln\left(\frac{cmc_1}{cmc_2}\right) = B_1 + B_2 \tag{12d}$$

where B_0 is a constant taken as − 7.80; the calculated values of B_1, B_2 and ΔG_{M} can be obtained in Table 3. With the decrease of x_1 in the mixed systems, the values of ΔG_{M} are decrease correspondingly as visualized in Fig. 6, that is, forming the stable mixed micelles. The minimum ΔG_{M} value is − 21.42 KJ/mol when x_1 is 0.2, due to the interaction between CTAB and $F_9EG_{13}F_9$. Adding a small CTAB amount to $F_9EG_{13}F_9$ can favor the formation of compact mixed micelles owing to the decrease of steric hindrance effect. But with the increase of CTAB component, the mutual immiscibility between the hydrocarbon and fluorocarbon surfactants increases, which is adverse for the closely arrangement of surfactant molecules in the mixed micelles.

3.4 Wettability of binary mixtures

Wettability is a significant property for surfactants, which enables them to be widely used for industrial production and daily life [40–42]. Generally speaking, the wettability of surfactants is directly related to their contact angle on a solid surface, that is, the smaller contact angle and the better wettability. Therefore, the contact angle measurements were conducted to evaluate the wettability of individual CTAB, $F_9EG_{13}F_9$ and their mixtures on PTFE film and parafilm, respectively.

It is described in Fig. 7a and b that the contact angles of CTAB/$F_9EG_{13}F_9$ mixtures on PTFE and parafilm decrease with the increase of time. Figure 7c and d present the variation images of solution droplet of binary mixture (x_1 = 0.6) within 100 s. From Fig. 7a, it can be found that introducing $F_9EG_{13}F_9$ to CTAB effectively decreases the contact angle of CTAB and the more composition of $F_9EG_{13}F_9$, the smaller contact angle of surfactant solution. This is caused by the low surface energy of $F_9EG_{13}F_9$ and the synergistic interaction between two surfactants. When the x_1 decreases from 1 to 0.6, the surfactant mixtures possess lower contact angle than $F_9EG_{13}F_9$ before about 35 s, indicating that these

Table 3 Thermodynamic parameters for CTAB/$F_9EG_{13}F_9$ mixtures at different CTAB proportions at 25 °C

x_1	ΔG_{mic} (KJ/mol)	ΔG_{ads} (KJ/mol)	ΔG (KJ/mol)	ΔG_{ideal} (KJ/mol)	B_1	B_2	ΔG_{M} (KJ/mol)
1	−29.14	−61.11	–	–	–	–	–
0.8	−29.91	−63.45	−2.37	−1.55	−1.48	1.53	−20.08
0.6	−30.06	−65.16	−2.59	−1.71	− 1.39	1.44	−20.16
0.4	−30.38	−65.52	−2.88	−1.70	−1.88	1.93	−20.47
0.2	−31.14	−63.72	−3.76	−1.64	− 3.61	3.66	−21.42
0	−29.26	−41.31	–	–	–	–	–

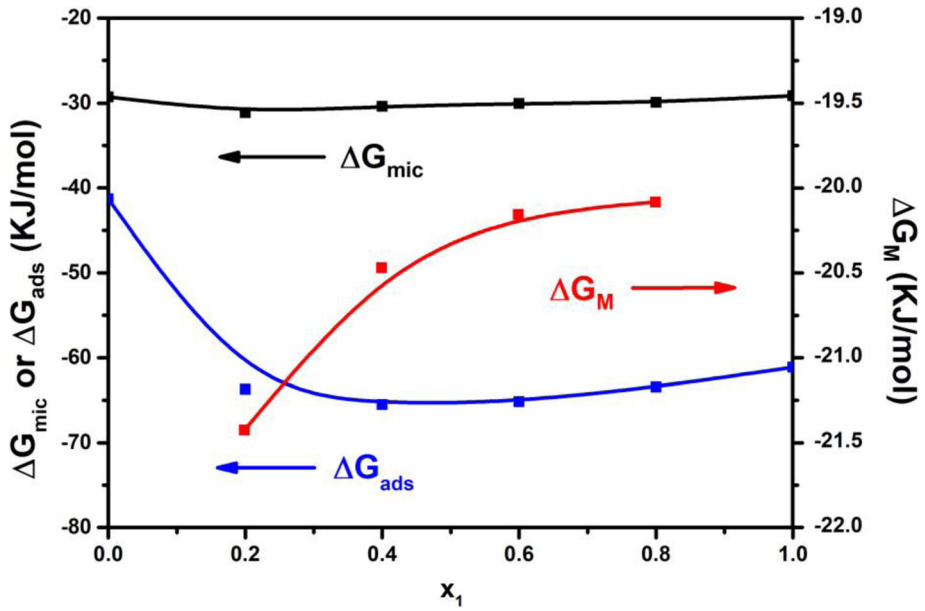

Fig. 6 Variation of thermodynamic parameters with the molar fraction of CTAB at 25 °C in aqueous solutions

surfactant mixtures easier migrate from solution to liquid-solid surface due to the decrease of steric hindrance effect and electrostatic repulsion effect. Surprisingly, the contact angle of binary surfactant mixture at $x_1 = 0.2$ can reduce to 57.7 ° at 100 s which is lower than that of $F_9EG_{13}F_9$ (73.8 °), that is, the wettability of binary surfactant mixtures is even better than that of $F_9EG_{13}F_9$ at a low x_1. Similar results can be found in Fig. 7b, further suggesting the superior wettability of CTAB/$F_9EG_{13}F_9$ mixtures. However, for parafilm, the wettability

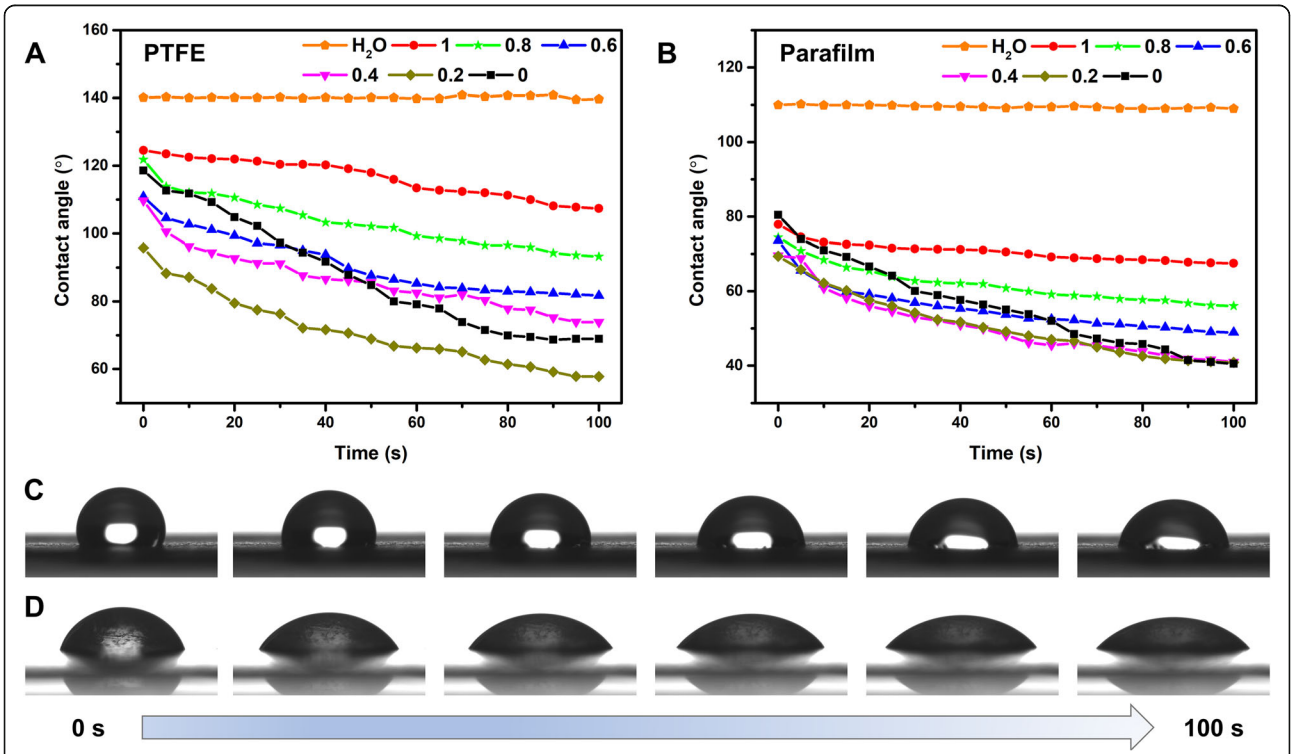

Fig. 7 a-b Dynamic contact angle of 1 mmol/L CTAB/$F_9EG_{13}F_9$ mixtures at different proportion of CTAB at 25 °C in aqueous solutions on **a** PTFE film and **b** parafilm. **c-d** Variation images of solution droplet of 1 mmol/L CTAB/$F_9EG_{13}F_9$ mixture (x_1 = 0.6) at 25 °C on **c** PTFE film and **d** parafilm

of binary mixtures is preferable to that of $F_9EG_{13}F_9$ when the x_1 reaches 0.4. This difference may be related to the property of parafilm whose higher surface energy enables binary surfactant mixtures to easily spread on the solid surface.

3.5 Colloidal stability of binary mixtures

Colloidal stability is another important factor that determines the commercial value of these surfactant mixtures. Fig. 8 is the visualized image of samples and unveils the difference between CTAB/$F_9EG_{13}F_9$ mixtures with x_1 = 1, 0.6 and 0 on the colloidal stability. For CTAB (x_1 = 1), its solution is very transparent and there is almost no Tyndall effect due to the small size of aggregates [43]. With the increase of time, the solution properties have no obvious change. For CTAB/$F_9EG_{13}F_9$ mixture (x_1 = 0.6), its solution is transparent blue and the Tyndall effect can be seen obviously. After 7 days, there is no significant change in the red beam path and transparency of solution, verifying the good colloidal stability of surfactant mixture. As for $F_9EG_{13}F_9$ (x_1 = 0), its solution is slightly cloudy and the incident light cannot pass through the solution well indicating the formation of large aggregates. After 3 days, the transparency of solution increases and the red beam path can also be found but not obvious. After a week, the transparency of the solution further increases and the red beam path basically disappears. Figure 9 unveils the transmittance spectra of these samples. It can be found that the variation trend of transmittance of solutions agree well with the above description. A possible explanation for the transmittance variation of $F_9EG_{13}F_9$ solution is the weak interaction between the aggregates. Because of the hydrophilic shell of aggregates constituted by the nonionic polyoxyethylene chains, these aggregates of $F_9EG_{13}F_9$ are easy to further gather together and turn into white precipitate at the bottom of the vial (as exhibited in Fig. 8). The addition of CTAB provides a certain positive charge for the hydrophilic shell of aggregates and increases the electrostatic repulsion effect between the aggregates favoring the stable dispersion of the aggregates in solution.

3.6 Solubilization of hydrophobic dye

Solubilization effect of surfactants on hydrophobic organic compounds is important because these organic compounds are usually harmful and difficult to remove from environment. Surfactants can form micelles in aqueous solution, when the concentration is larger than *cmc*. The micelle has a hydrophilic shell and hydrophobic core which can incorporate these hydrophobic organic compounds in water, thereby improving their

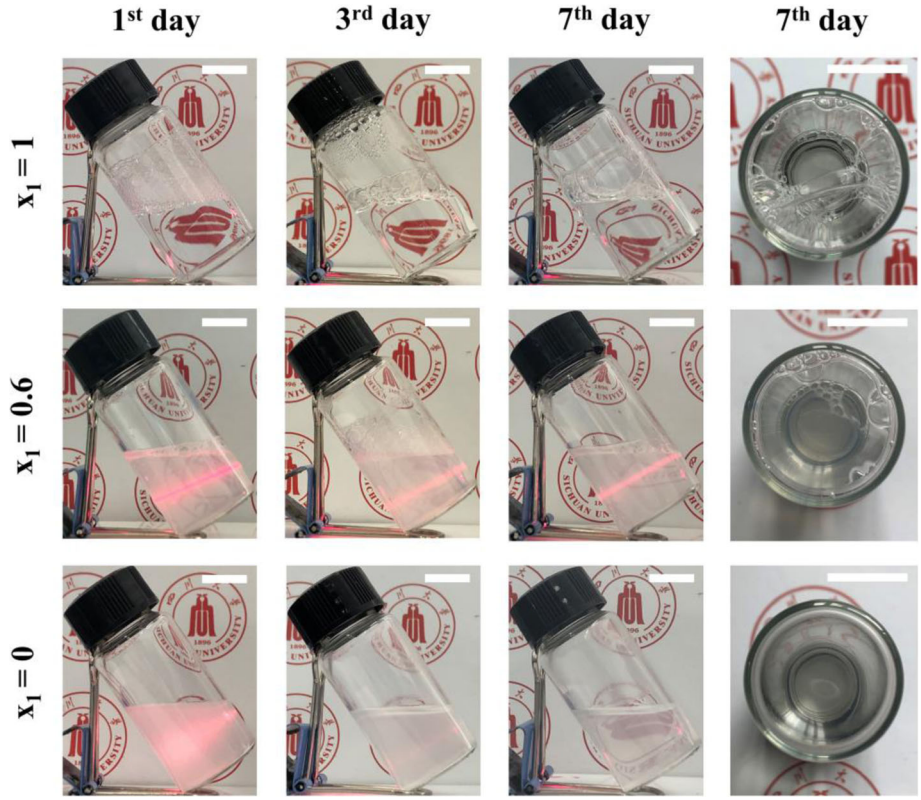

Fig. 8 Digital photographs of samples of 2.5 mmol/L CTAB/$F_9EG_{13}F_9$ mixtures (x_1 = 1, 0.6 and 0) at 25 °. Scale bars in digital photos are 1 cm

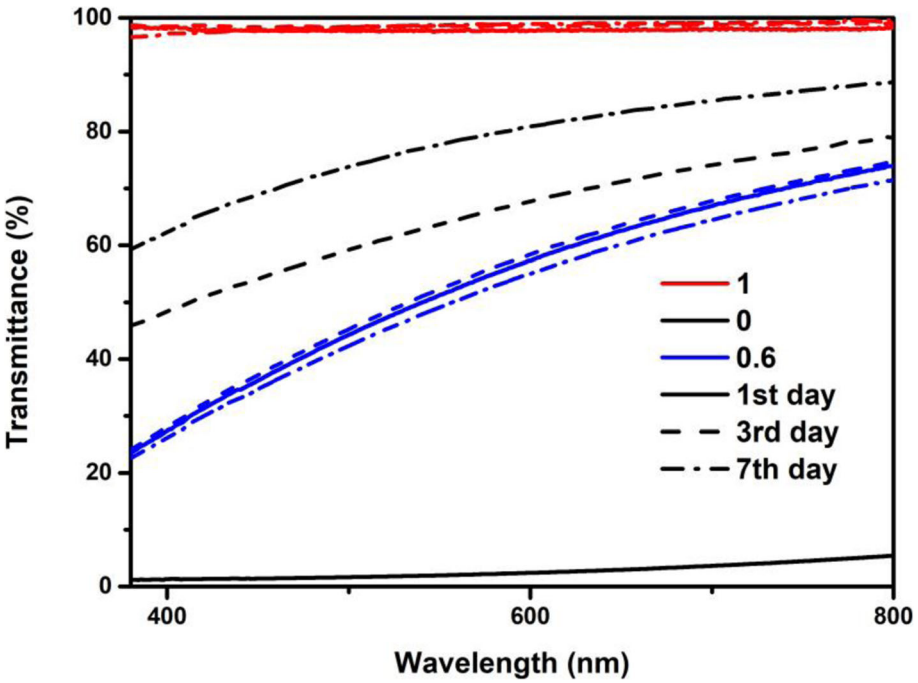

Fig. 9 Transmittance spectra of samples of 2.5 mmol/L CTAB/$F_9EG_{13}F_9$ mixtures (x_1 = 1, 0.6 and 0) at 25 °

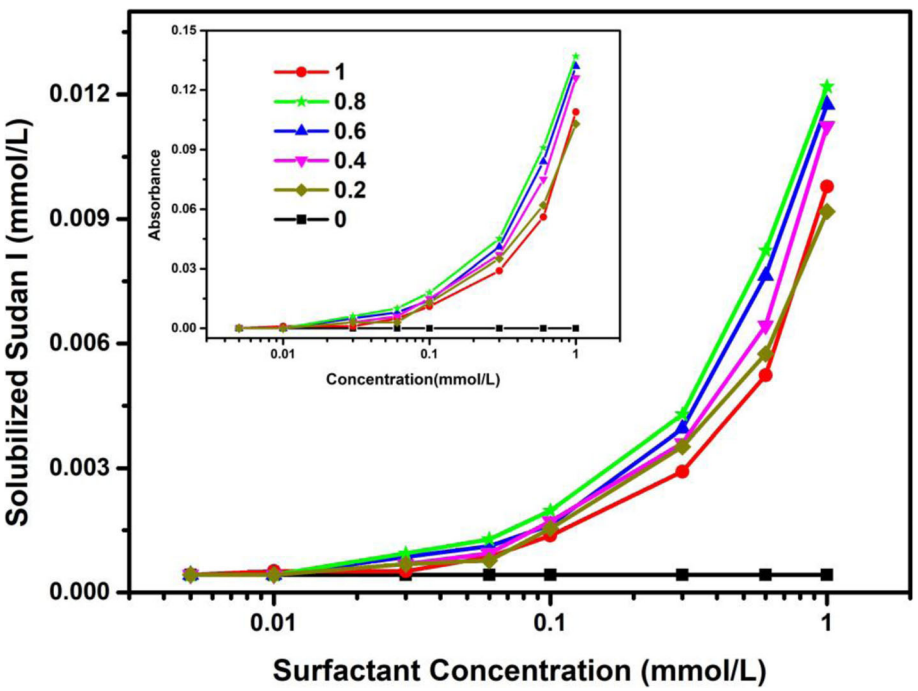

Fig. 10 Solubility of Sudan I in CTAB/$F_9EG_{13}F_9$ mixtures as a function of surfactant concentration at 25 °C. The inset is absorbance of Sudan I in CTAB/$F_9EG_{13}F_9$ mixtures as a function of surfactant concentration at 25 °C

solubility. Generally speaking, resulting in the lack of solubilization ability towards hydrocarbons of fluorocarbon surfactants, these hydrophobic substances are hydrocarbons which have poor compatibility with fluorocarbon surfactants [44].

Mixing hydrocarbon surfactants with fluorocarbon surfactants may be an effectively method to solve this problem due to the formation of mixed micelles. Herein, the solubilization of CTAB/$F_9EG_{13}F_9$ mixtures towards hydrophobic dye (Sudan I) was investigated by a UV-Visible spectrophotometer. The absorbance curves of Sudan I versus concentration of binary surfactant mixtures with different x_1 are depicted in Fig. 10 inset. It can be obviously seen that the absorbance increases with the increase of surfactant concentration. When the concentration exceeds a specific value, the absorbance increases shapely due to the formation of micelle. To further assess the solubilization ability of binary surfactant mixtures, the concentration of solubilized Sudan I is calculated according to the molar absorption coefficient and disclosed in Fig. 10. The molar solubilization power (SP_M) of different mixed systems can be obtained according to the following relationship [45].

$$SP_M = \frac{S_{dye} - S_{cmc}}{C_s - cmc} \tag{13}$$

where S_{dye} and S_{cmc} are the solubility of Sudan I in the solution at a particular surfactant concentration or at critical micelle concentration, respectively; C_s is the concentration of CTAB/$F_9EG_{13}F_9$ mixtures. The calculated results can be found in Table 4. It points out that CTAB has a larger SP_M value (0.00913) than that of $F_9EG_{13}F_9$ (0), which means a better solubilization ability. Compared with CTAB, $F_9EG_{13}F_9$ hardly solubilizes Sudan I due to the mutual immiscibility of hydrocarbon and fluorocarbon compounds. In fact, some similar results can be found in other literatures. For example, Takata et al. [46] found individual fluorocarbon surfactant hardly solubilizes Sudan III and Matsuoka et al. [44] reported that a series of fluorocarbon surfactants had no solubilization ability towards naphthalene. As a result, fluorocarbon surfactants are unlikely to have applications in the solubilization of hydrocarbons.

Table 4 Solubilization parameters for CTAB/$F_9EG_{13}F_9$ mixtures at different CTAB proportions at 25 °C

x_1	SP_M	SP_{ideal}	lnK_m	ΔG_s (KJ/mol)
1	0.00913	0.00913	4.78	−11.84
0.8	0.01195	0.00730	5.02	−12.44
0.6	0.01149	0.00548	5.10	−12.64
0.4	0.01068	0.00365	5.23	−12.95
0.2	0.00883	0.00183	5.42	−13.43
0	0	0	–	–

In our experiment, when adding a small CTAB amount, the solubilization ability of $F_9EG_{13}F_9$ is effectively improved. For example, the SP_M value of CTAB/$F_9EG_{13}F_9$ mixture at x_1 = 0.2 is 0.00883, which is close to that of CTAB. This is caused by the fact that the formation of mixed micelle improves the compatibility of heterogeneous system and favors the insertion of Sudan I. Besides, the lower *cmc* value of this binary mixture also endows it with a stronger solubilization ability than $F_9EG_{13}F_9$. With further increasing x_1, the SP_M values increase correspondingly. The maximum SP_M is 0.01195 when x_1 = 0.8, which is even larger than that of CTAB. Above results further indicate that mixed surfactant systems possess a better solubilization ability than individual CTAB or $F_9EG_{13}F_9$.

For an ideal mixed surfactant system, their SP_M values can be calculated by following relationship [47].

$$SP_{ideal} = x_1 SP_M^1 + (1 - x_1) SP_M^2 \tag{14}$$

where SP_{ideal} is the ideal SP_M value of binary surfactant mixture; SP_M^1 and SP_M^2 denote the SP_M value of individual CTAB and $F_9EG_{13}F_9$, respectively. The SP_{ideal} values of CTAB/$F_9EG_{13}F_9$ mixtures with different x_1 are presented in Table 4. A positive deviation of the experimental value from the ideal one can be found in Fig. 11, further suggesting the non-ideal behavior of mixtures and verifying the strong synergistic effect between CTAB and $F_9EG_{13}F_9$.

In addition, the partition coefficient of Sudan I between mixed micelle phase and aqueous phase (K_m) and the standard free energy of solubilization (ΔG_s) can be used to estimate the trend of solubilization [48, 49].

$$K_m = 55.4 \times \frac{SP_M}{[S_{cmc}(1 + SP_M)]} \tag{15}$$

$$\Delta G_s = -RT \ \ln K_m \tag{16}$$

The lnK_m and ΔG_s values are listed in Table 4. Specially, the lnK_m and ΔG_s values of $F_9EG_{13}F_9$ cannot be given in this work due to the S_{cmc} = 0. From Table 4, the lnK_m values increase with the decrease of x_1 and the maximum lnK_m value is 5.42 at x_1 = 0.2. This is because the *cmc* value reach minimum when x_1 = 0.2, which favors the insertion of Sudan I. However, this is not consistent with the SP_M indicating that the solubilization ability is related to not only *cmc* but also micellar composition. The calculated ΔG_s values are all negative suggesting the spontaneous solubilization process.

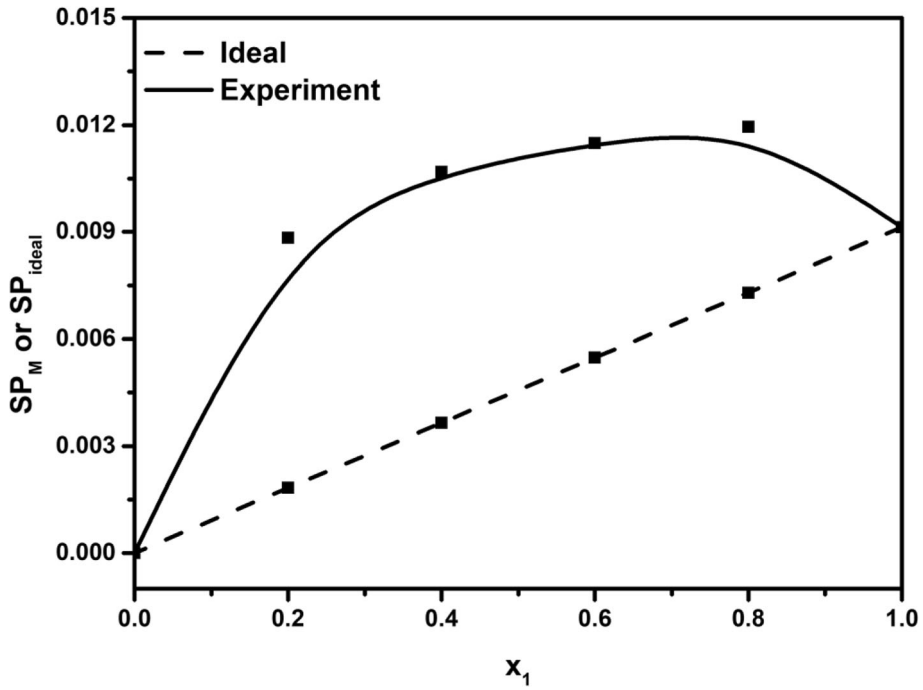

Fig. 11 Comparison between the experimental and ideal SP_M values of binary surfactant mixtures at different CTAB proportions at 25 °C

4 Conclusions

In conclusion, the micellization, adsorption, thermodynamics, wettability, colloidal stability and solubilization towards Sudan I of CTAB/$F_9EG_{13}F_9$ mixtures were investigated successively based on different theoretical models and experimental methods. The results manifested that mixing CTAB with $F_9EG_{13}F_9$ is non-ideal and a strong synergistic effect exists in these mixtures. Among them, CTAB/$F_9EG_{13}F_9$ mixture at x_1 = 0.2 had the strongest synergistic effect (β_{12} = − 3.662). Its *cmc* and surface tension could reach 0.191 mmol/L and 22.7 mN/m, respectively. Besides, the contact angle of this surfactant mixture could reduce to 57.7 ° at 100 s, which is even lower than $F_9EG_{13}F_9$. Compared with $F_9EG_{13}F_9$, CTAB/$F_9EG_{13}F_9$ mixtures also presented a better colloidal stability. In addition, introducing CTAB into $F_9EG_{13}F_9$ effectively improved the solubilization ability towards Sudan I of $F_9EG_{13}F_9$ where the SP_M value of CTAB/$F_9EG_{13}F_9$ mixture at 0.4 (0.01068) even exceeded that of CTAB (0.00913). Based on the results mentioned above, CTAB/$F_9EG_{13}F_9$ mixtures could be widely used in practical applications as a feasible alternative for individual $F_9EG_{13}F_9$ because of their better performances and lower used cost.

Acknowledgments

This work was financially supported by the National Natural Science Foundation of China (No. 22078207), the Sichuan Science and Technology Program (2021ZHCG0042) and the Fundamental Research Funds for the Central Universities (China). The authors would thank Zhonghui Wang and Qingshuang Song (College of Biomass Science and Engineering, Sichuan University) for their help in DLS and contact angle measurements.

Authors' contributions

YZ and YJ conceived and designed the study. YZ and YT performed the experiments and analyzed the experiments data. YJ, YS, LS and SL reviewed and edited the manuscript. All authors read and approved the manuscript.

Funding

National Natural Science Foundation of China (No. 22078207); Sichuan Science and Technology Program (2021ZHCG0042); Fundamental Research Funds for the Central Universities (China).

Availability of data and materials

All data generated or analyzed during this study are included in this published article. The authors declare that the data in this article is reliable.

Declaration

Competing interests

The authors declare that they have no competing interests.

Received: 22 March 2021 Accepted: 10 June 2021
Published online: 15 September 2021

References

1. Zhou R, Jin Y, Shen Y, Zhao P, Zhou Y. Synthesis and application of non-bioaccumulable fluorinated surfactants: a review. J Leather Sci Eng. 2021; 3(1):6. https://doi.org/10.1186/s42825-020-00048-7.
2. Shen Y, Jin Y, Lai S, Shi L, Zhou Y, Zhou R. Nonionic short-chain fluorinated surfactants in fatliquoring of chrome-tanned goat skin. J Am Leather Chem As. 2020;115(7):255–62.
3. Liu S, Qiu-feng AN, Wei XU. Synthesis and application fluorinated polyacrylate emulsifier-free emulsion. Leather Sci Eng. 2011;21(5):46–50 (in Chinese).
4. Glüge J, Scheringer M, Cousins IT, DeWitt JC, Goldenman G, Herzke D, et al. An overview of the uses of per- and polyfluoroalkyl substances (PFAS).

Environ Sci: Processes Impacts. 2020;22(12):2345–73. https://doi.org/10.1039/d0em00291g.
5. Krafft MP, Riess JG. Per- and polyfluorinated substances (PFASs): environmental challenges. Curr Opin Colloid Interface Sci. 2015;20(3):192–212. https://doi.org/10.1016/j.cocis.2015.07.004.
6. Lindstrom AB, Strynar MJ, Libelo EL. Polyfluorinated compounds: past, present, and future. Environ Sci Technol. 2011;45(19):7954–61. https://doi.org/10.1021/es2011622.
7. Kostov G, Boschet F, Ameduri B. Original fluorinated surfactants potentially non-bioaccumulable. J Fluor Chem. 2009;130(12):1192–9. https://doi.org/10.1016/j.jfluchem.2009.08.002.
8. Segal L, Philips FJ, Loeb L, Clayton RL. Oil and water repellent treatments for cotton with fluorochemicals1. Text Res J. 1958;28(3):233–41. https://doi.org/10.1177/004051755802800308.
9. Sha M, Xing P, Jiang B. Strategies for synthesizing non-bioaccumulable alternatives to PFOA and PFOS. Chin Chem Lett. 2015;26(5):491–8. https://doi.org/10.1016/j.cclet.2015.03.038.
10. Verdia P, Gunaratne HQN, Goh TY, Jacquemin J, Blesic M. A class of efficient short-chain fluorinated catanionic surfactants. Green Chem. 2016;18(5):1234–9. https://doi.org/10.1039/C5GC02790J.
11. E-k K, Jung GY, Jung SH, Lee BM. Synthesis and surface active properties of novel anionic surfactants with two short fluoroalkyl groups. J Ind Eng Chem. 2018;61:216–26.
12. Wang R, Song L, Guo Y, Kou J, Song H, Liu Y, et al. Synthesis and structure–activity relationships of nonionic surfactants with short fluorocarbon chains. J Mol Liq. 2021;321:114486. https://doi.org/10.1016/j.molliq.2020.114486.
13. Shen Y, Jin Y, Lai S, Shi L, Du W, Zhou R. Synthesis, surface properties and cytotoxicity evaluation of nonionic urethane fluorinated surfactants with double short fluoroalkyl chains. J Mol Liq. 2019;296:111851. https://doi.org/10.1016/j.molliq.2019.111851.
14. Zhou R, Jin Y, Shen Y, Lai S, Zhou Y, Zhao P. Surface activity, salt and pH tolerance, and wettability of novel nonionic fluorinated surfactants with a short fluorocarbon chain. J Dispers Sci Technol. 2020;42(1):152–9. https://doi.org/10.1080/01932691.2020.1768862.
15. Banerjee S, Schmidt J, Talmon Y, Hori H, Asai T, Ameduri B. A degradable fluorinated surfactant for emulsion polymerization of vinylidene fluoride. Chem Commun. 2018;54(81):11399–402. https://doi.org/10.1039/C8CC05290E.
16. Zaggia A, Ameduri B. Recent advances on synthesis of potentially non-bioaccumulable fluorinated surfactants. Curr Opin Colloid Interface Sci. 2012;17(4):188–95. https://doi.org/10.1016/j.cocis.2012.04.001.
17. Ren ZH. Interacting behavior between amino sulfonate surfactant and octylphenol polyoxyethylene ether in aqueous solution and effect of hydrophilicity. Ind Eng Chem Res. 2014;53(24):10035–40. https://doi.org/10.1021/ie5011542.
18. Rehman A, Usman M, Bokhari TH, Rahman HMAU, Mansha A, Siddiq M, et al. Effects of nonionic surfactant (TX-100) on solubilizing power of cationic surfactants (CTAB and CPC) for direct red 13. Colloids Surf A Physicochem Eng Asp. 2020;586:124241. https://doi.org/10.1016/j.colsurfa.2019.124241.
19. Liu X, Lu Y, Luo G. Continuous flow synthesis of polystyrene nanoparticles via emulsion polymerization stabilized by a mixed nonionic and anionic emulsifier. Ind Eng Chem Res. 2017;56(34):9489–95. https://doi.org/10.1021/acs.iecr.7b02352.
20. Szymczyk K, González-Martín ML, Bruque JM, Jańczuk B. Effect of two hydrocarbon and one fluorocarbon surfactant mixtures on the surface tension and wettability of polymers. J Colloid Interface Sci. 2014;417:180–7. https://doi.org/10.1016/j.jcis.2013.11.033.
21. Assaker K, Stébé M-J, Blin J-L. Mesoporous silica materials from diluted and concentrated solutions of nonionic fluorinated and ionic hydrogenated surfactants mixtures. Colloids Surf A Physicochem Eng Asp. 2018;536:242–50. https://doi.org/10.1016/j.colsurfa.2017.02.056.
22. Zhang J, Pi B, Wang X, Yang Z, Lv Q, Lin M. Formation of polyhedral vesicle gels from catanionic mixtures of hydrogenated and perfluorinated surfactants: effect of fluoro-carbon alkyl chain lengths. Soft Matter. 2018;14(40):8231–8. https://doi.org/10.1039/C8SM01787E.
23. Wang G, Yin Q, Shen J, Bai Y, Ma X, Du Z, et al. Surface activities and aggregation behaviors of cationic - anionic fluorocarbon - hydrocarbon surfactants in dilute solutions. J Mol Liq. 2017;234:142–8. https://doi.org/10.1016/j.molliq.2017.03.059.
24. Zhang D, Bai Y, Shen J, Wang G. Surface activities and wetting behavior of fluorocarbon-cationic and hydrocarbon-anionic surfactant mixtures in dilute solutions. J Mol Liq. 2019;286:110947. https://doi.org/10.1016/j.molliq.2019.110947.
25. Jiang N, Sheng Y, Li C, Lu S. Surface activity, foam properties and aggregation behavior of mixtures of short-chain fluorocarbon and hydrocarbon surfactants. J Mol Liq. 2018;268:249–55. https://doi.org/10.1016/j.molliq.2018.07.055.
26. Pashirova TN, Ziganshina AY, Sultanova ED, Lukashenko SS, Kudryashova YR, Zhiltsova EP, et al. Supramolecular systems based on calix[4]resorcine with mono-, di-, and tetracationic surfactants: synergetic structural and solubilization behavior. Colloids Surf A Physicochem Eng Asp. 2014;448:67–72. https://doi.org/10.1016/j.colsurfa.2014.02.012.
27. Zhou Q, Rosen MJ. Molecular interactions of surfactants in mixed monolayers at the air/aqueous solution interface and in mixed micelles in aqueous media: the regular solution approach. Langmuir. 2003;19(11):4555–62. https://doi.org/10.1021/la020789m.
28. Chen C, Wang S, Tian W, Wang S, Shiau B-J, Harwell JH. Micellar interaction of binary mixtures of alpha olefin sulfonate and nonylphenol polyethylene glycol ethers: length effects of ethylene oxide. Colloids Surf A Physicochem Eng Asp. 2018;542:31–41. https://doi.org/10.1016/j.colsurfa.2018.01.036.
29. Ren ZH, Huang J, Luo Y, Zheng YC, Mei P, Lai L, et al. Micellization behavior of binary mixtures of amino sulfonate amphoteric surfactant with different octylphenol polyoxyethylene ethers in aqueous salt solution: both cationic and hydrophilic effects. Ind Eng Chem Res. 2016;36:263–70. https://doi.org/10.1016/j.jiec.2016.02.009.
30. Akbaş H, Kasapoğlu S, Boz M. Aggregation behavior and intermolecular interaction of binary surfactant mixtures based on cationic Geminis and nonionic surfactants. Colloid Polym Sci. 2015;293(12):3429–37. https://doi.org/10.1007/s00396-015-3702-9.
31. Kabir ud D, Sharma G, Naqvi AZ. Micellization and interfacial behavior of binary surfactant mixtures based on cationic geminis and nonionic tweens. Colloids Surf A Physicochem Eng Asp. 2011;385(1):63–71. https://doi.org/10.1016/j.colsurfa.2011.05.053.
32. Clint JH. Micellization of mixed nonionic surface active agents. J Chem Soc Faraday Trans. 1975;71(0):1327–34. https://doi.org/10.1039/f19757101327.
33. Rubingh DN. Mixed micelle solutions, solution chemistry of surfactants. Boston: Springer; 1979. https://doi.org/10.1007/978-1-4615-7880-2_15.
34. Sis H, Chander G, Chander S. Synergism in sodium oleate/ethoxylated nonylphenol mixtures. J Dispers Sci Technol. 2005;26(5):605–14. https://doi.org/10.1081/DIS-200057666.
35. Chaudhuri RG, Sunayana S, Paria S. Wettability of a PTFE surface by cationic–non-ionic surfactant mixtures in the presence of electrolytes. Soft Matter. 2012;8(20):5429–33. https://doi.org/10.1039/c2sm25309g.
36. Rosen MJ, Fei L, Zhu Y-P, Morrall SW. The relationship of the environmental effect of surfactants to their interfacial properties. J Surfactant Deterg. 1999;2(3):343–7. https://doi.org/10.1007/s11743-999-0087-2.
37. Rosen M, Junkappu JT. Surfactants and interfacial phenomena. 4rd ed. Hoboken: Wiley-Interscience; 2012. https://doi.org/10.1002/9781118228920.
38. Rosen MJ, Aronson S. Standard free energies of adsorption of surfactants at the aqueous solution/air interface from surface tension data in the vicinity of the critical micelle concentration. Colloids Surf. 1981;3(3):201–8. https://doi.org/10.1016/0166-6622(81)80037-6.
39. Maeda H. A simple thermodynamic analysis of the stability of ionic/nonionic mixed micelles. J Colloid Interface Sci. 1995;172(1):98–105. https://doi.org/10.1006/jcis.1995.1230.
40. Lin J, Wang W, Bai W, Zhu M, Zheng C, Liu Z, et al. A gemini-type superspreader: synthesis, spreading behavior and superspreading mechanism. Chem Eng J. 2017;315:262–73. https://doi.org/10.1016/j.cej.2016.12.132.
41. Li J, Bai Y, Wang W, Tai X, Wang G. Green Glucamine-based trisiloxane surfactant: surface activity, aggregate behavior, and superspreading on hydrophobic surfaces. ACS Sustain Chem Eng. 2019;7(4):4390–8. https://doi.org/10.1021/acssuschemeng.8b06282.
42. Babu K, Pal N, Bera A, Saxena VK, Mandal A. Studies on interfacial tension and contact angle of synthesized surfactant and polymeric from castor oil for enhanced oil recovery. Appl Surf Sci. 2015;353:1126–36. https://doi.org/10.1016/j.apsusc.2015.06.196.
43. Kang C, Wu J, Zheng Y, Lai L. Studies on the surface properties and microaggregates of cationic/anionic surfactant mixtures based on sulfonate gemini surfactant. J Mol Liq. 2020;320:114431. https://doi.org/10.1016/j.molliq.2020.114431.
44. Matsuoka K, Yamashita R, Ichinose M, Kondo M, Yoshimura T. Solubilization of naphthalene and octafluoronaphthalene in ionic hydrocarbon and fluorocarbon surfactants. Colloids Surf A Physicochem Eng Asp. 2014;456:83–91. https://doi.org/10.1016/j.colsurfa.2014.04.060.

45. Tehrani-Bagha AR, Singh RG, Holmberg K. Solubilization of two organic dyes by anionic, cationic and nonionic surfactants. Colloids Surf A Physicochem Eng Asp. 2013;417:133–9. https://doi.org/10.1016/j.colsurfa.2012.10.006.
46. Takata Y, Ohtsuka Y, Ashida T. Effect of hydrophobic chains on solubilization of hydrocarbon and fluorocarbon surfactant mixtures in aqueous solution. J Oleo Sci. 2019;68(9):855–61. https://doi.org/10.5650/jos.ess19086.
47. Wei J, Huang G, Yu H, An C. Efficiency of single and mixed Gemini/conventional micelles on solubilization of phenanthrene. Chem Eng J. 2011;168(1):201–7. https://doi.org/10.1016/j.cej.2010.12.063.
48. Long J, Li L, Jin Y, Sun H, Zheng Y, Tian S. Synergistic solubilization of polycyclic aromatic hydrocarbons by mixed micelles composed of a photoresponsive surfactant and a conventional non-ionic surfactant. Sep Purif Technol. 2016;160:11–7. https://doi.org/10.1016/j.seppur.2016.01.010.
49. Liu J, Wang Y, Li H. Synergistic solubilization of phenanthrene by mixed micelles composed of biosurfactants and a conventional non-ionic surfactant. Molecules. 2020;25(18):4327. https://doi.org/10.3390/molecules25184327.

Publisher's Note